# Journal of Agrometeorology

*ISSN : 0972-1665 (print), 2583-2980 (online)*
*Vol. No. 24 (4) : 335-347 (December- 2022)*

*https://journal.agrimetassociation.org/index.php/jam*


***Research Paper***

# Impact of dynamic vegetation on near-surface meteorology using a newly developed WRF_NOAHMP_SUCROS coupled model


**SARITA KUMARI* and S. BAIDYA ROY**

*Centre for Atmospheric Sciences, Indian Institute of Technology Delhi, New Delhi 110016*
**Corresponding author email: saritaladoiya@gmail.com*



**ABSTRACT**

The study attempts to quantitatively understand the impact of dynamic vegetation on land-surface atmosphere interactions over spring wheat croplands in India. A new modeling tool capable of simulating these interactions was developed by incorporating the crop growth module of the Simple and Universal Crop growth Simulator (SUCROS) crop model into the Weather Research and Forecasting (WRF) mesoscale model. An earlier study had calibrated and evaluated the stand-alone SUCROS crop model with observed data for spring wheat collected from an experimental site in northwestern India. The crop growth module of the calibrated SUCROS model was implemented in the Noah-MP land module of WRF to build the coupled WRF_NOAHMP_SUCROS model. Numerical experiments were conducted with WRF_SUCROS that simulates the simultaneous evolution of meteorological drivers and crop Leaf Area Index (LAI) and the two-way interactions between these processes. These experiments were compared with WRF simulations driven by observed climatological mean LAI. These experiments only simulate the effects of changes in LAI on meteorology but not the other round. Results show that the coupled WRF_NOAHMP_SUCROS model is able to simulate the LAI better than the default dynamic vegetation module in WRF. It also produces realistic simulations of the near-surface meteorological parameters. The latent heat flux (LHF) varies directly with LAI, and sensible heat flux (SHF) varies inversely with LAI. As the crop grows, the energy transfer occurs more in latent heat flux than sensible heat flux due to increased evapotranspiration. Hence the growing crops result in near-surface cooling due to decreased Bowed Ratio. The mixing ratio is also increased due to increased latent heat flux. The uncoupled WRF model also shows similar patterns except in the juvenile crop stage where it overestimates the sensible heating and temperature but underestimates latent heat fluxes and mixing ratio.



***Keywords***: Crop model, SUCROS, Noah-MP, coupled, spring wheat


Land and atmosphere are tightly coupled parts of the Earth System. Changes in land surface properties, e.g., surface temperature, surface albedo, vegetation type and phenology, soil moisture etc., influence weather and climate by changing carbon, water, momentum and energy fluxes. The weather and climate effects can occur at a wide range of spatial-temporal scales (Pielke *et al*., 1998; Avissar; Verstraete, 1990), which can vary from local to regional to global scales in space and from hours to centuries in time (Pitman, 2003; Sellers, 1992).

Land-use and land cover changes have influenced the present and future climate (Scanlon *et al.*, 2005; Twine *et al*., 2004; DeFries *et al.,* 2004 Lambin *et al.,* 2003; Foley *et al.,* 2003). An appropriate representation of the land surface is essential to ensure high-quality simulation of land-atmosphere interactions. Vegetation is a necessary part of the land surface that strongly contributes to the exchange of moisture, heat, and momentum fluxes between the land surface and the atmosphere.

The interaction between vegetation and the atmosphere can occur in two ways: the first is a one-way interaction, and the second is a two-way interaction.

One-way interaction studies on croplands reflect either the effects of meteorology on crops or the effects of dynamic crops on meteorology. Kumari *et al.* (2019) and Pandey *et al.* (2007) have shown the impact of different meteorological parameters on wheat crop growth using the SUCROS and CERES-Wheat models. Hatfield (2015) and Asseng *et al*. (2015) have studied the impact


***Article info - DOI***: *https://doi.org/10.54386/jam.v24i4.1892*
*Received: 16 Octotber 2022; Accepted: 18 November 2022; Published online : 1 December 2022*

of temperature on vegetation growth and yield. Hundal and Kaur (2007) and Yao *et al.* (2007) used different crop models to study the effects of climate change on crop growth and production of crops. Hatfield *et al.* (2011) have shown the impact of changing temperature, precipitation and $CO_2$ on crop production. In addition to the influence of meteorology on crop growth and crop production, some studies show an effect of dynamic crop growth on near-surface meteorology.

Sacks and Kucharik (2011) used the Agro-IBIS agroecosystem model to study the effects of various planting dates and crop growing degree day requirements on crop yield and fluxes of energy and water over the U.S. corn belt. Van den Hoof *et al*. (2011) used a JULES- SUCROS coupled model to simulate the impact of wheat phenology on fluxes at 6 European FLUXNET sites. Chen and Xie (2011) coupled the CERES crop model with Biosphere-Atmosphere Transfer Scheme (BATS) to study the land surface and crop growth interactions. Chen *et al.* (2020) calibrated and evaluated the SiBcrop model to accurately simulate the LAI, LHF and SHF of winter wheat used to grow in a double-cropping system in the plains of northern China.

If we talk about two-way interaction studies, there are some studies at a global scale (Henderson-Sellers and McGuffie, 1995; Foley *et al.,* 1998; Dan *et al*., 2005; and Bonan *et al*., 2003) and at regional scales (Lu *et al*., 2001; Campo *et a*l., 2009; Shin *et al.,* 2006) that represents the impact of crop dynamics on meteorology. Apart from these studies, few studies (Osborne *et al.,* 2009; Osborne *et al*., 2007; Tsvetsinskaya *et al*., 2001a; Liu *et al*., 2016; Lu *et al.*, 2015; Harding *et al.,* 2015; Zou *et al*., 2019; Jiang *et al*., 2009; and Tsarouchi *et al*., 2014) have shown two-way interactions using mesoscale models but at a coarse resolution.

There are only three mesoscale studies in this area, focusing on specific crops. They have developed models by coupling an atmospheric model like a crop model (Liu *et al*., 2016; Lu *et al*., 2015; and Tsvetsinskaya *et al.,* 2001a).

This study aims to quantitatively understand two-way interactions between vegetation and atmosphere over spring wheat croplands in India using a newly developed coupled crop-atmosphere model at a high resolution.

## MATERIALS AND METHODS

### *Models used*

The WRF model is a fully compressible and non-hydrostatic mesoscale model. The coupling was done by incorporating the calibrated SUCROS model as a Noah-MP land surface model module in WRF. Before going into a detailed discussion about the coupled model, let us look at the Noah-MP land surface and SUCROS crop models.

### *WRF Noah-MP land surface model*

The Noah-MP land surface model in the WRF is a new generation community land model implemented in the WRF model. The Noah-MP model provides a wide range of options to simulate physical processes occurring on the land surface. The Noah-MP model uses a photosynthesis scheme based on Ball-Berry stomatal resistance (Ball *et al.,* 1987), improved snow, surface heat fluxes, runoff, soil moisture and skin temperature modeling to determine land-atmosphere interactions. Noah-MP has a distinct vegetation canopy including crown radius, canopy top and bottom, and leaves having specified direction, dimensions, & density. The model deals with a two-stream radiation transfer scheme including shading effects to consider at the 3-dimensional structure of the canopy. Noah-MP has three snow layers that can melt/refreeze water and store liquid water. A snow interception model gives a detailed account of deposition/sublimation to and from snowpack (Niu and Yang, 2004; and Yang and Niu, 2003). The model has four soil layers with different soil depths (10, 30, 60, 100 cm thick) for maintaining soil moisture and heat fluxes, internal soil moisture and heat fluxes, interflow and gravitational flow. Based on input data, the Noah-MP module simulates soil temperature, skin temperature, soil moisture, snow depth, surface energy fluxes, canopy rainfall interception, water fluxes, $CO_2$ fluxes, canopy & vegetation temperature distribution, soil drainage and runoff (Niu *et al.,* 2011). The model also has dynamic characteristics of vegetation (Dickinson *et al.,* 1998) which uses multi-parameterization schemes. In the dynamic vegetation module of the Noah-MP model, there is an allocation of carbon to different parts of the plant. The model calculates photosynthesis for shaded and sunlit leaves with different rates. (Liu *et al*., 2016) The model uses predefined tables with some plant-specific parameters to control the various plant processes. The dynamic vegetation module of the Noah-MP model calculates the LAI for generic crops only, not for all the crops. This makes Noah-MP dynamic vegetation model incompatible for interaction studies.

### *SUCROS crop growth model*

The SUCROS crop growth model is a mechanistic model which computes crop growth depending on different plant processes under varying weather conditions. The potential growth of a crop is based on the rate of $CO_2$ assimilation that depends on temperature, incoming radiation, available soil moisture and LAI of the crop. The daily rate of gross $CO_2$ assimilation is computed from leaves' photosynthetic characteristics and radiation absorbed. Next, the net carbon assimilation is calculated by subtracting the respiratory losses from the gross assimilation. The net assimilated carbon is then partitioned among different parts of the plant (i.e., roots, leaves and shoots) depending on the different development stages of the plant. A detailed description of SUCROS crop model is given in Goudriaan and Van Laar (1994).

### *WRF_NOAHMP_SUCROS coupled model development*

The coupling is done by calling the SUCROS crop growth module by Noah-MP land surface model in the WRF mesoscale model. In the WRF_NOAHMP_SUCROS coupled model, the SUCROS subroutine is called by Noah-MP SFLX subroutine at a daily time step. In the WRF model, the plant growth is represented by the LAI and root depth. At the end of each day, the crop model calls various subroutines such as Leaf Assimilation, Total Assimilation, Growth, Water Stress and Root to simulate crop growth processes. The simulated leaf area index and root depth are fed back to the Noah-MP module at the end of each day. Noah-MP then calculates the soil moisture and land-atmosphere fluxes using the updated values of LAI and root depth. In this way, the coupled model works and accounts for the impact of crop growth on the atmosphere. A schematic diagram of the coupled WRF_NOAHMP_SUCROS dynamic crop model is shown in Fig. 1.

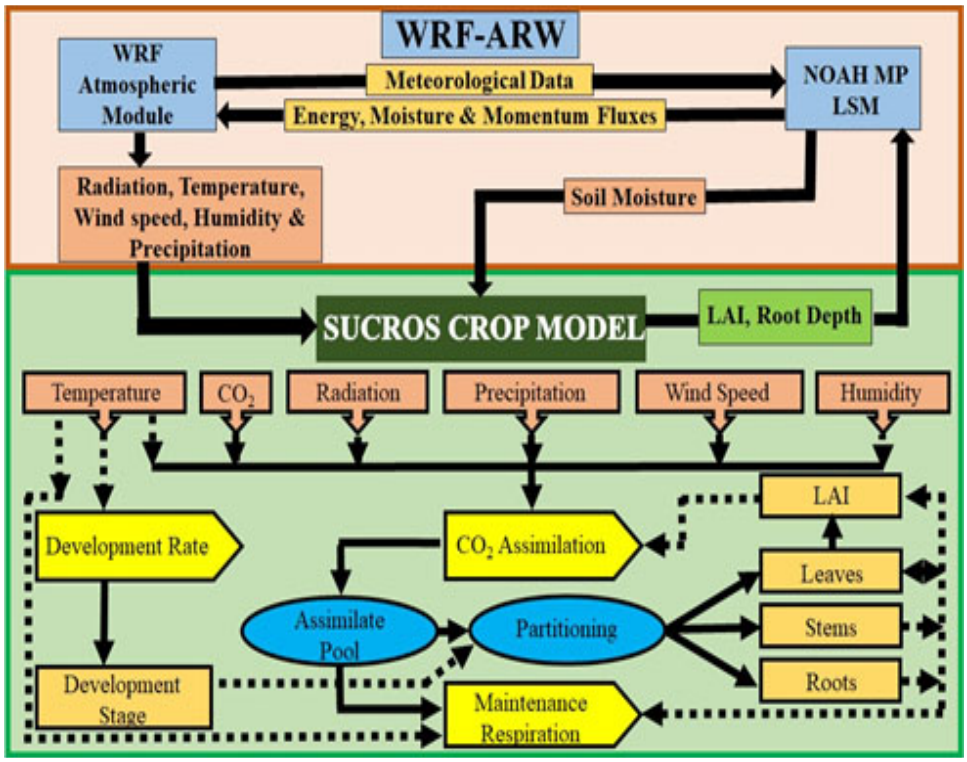


**Fig. 1:** Schematic diagram for coupled WRF_NOAHMP_SUCROS dynamic crop model.

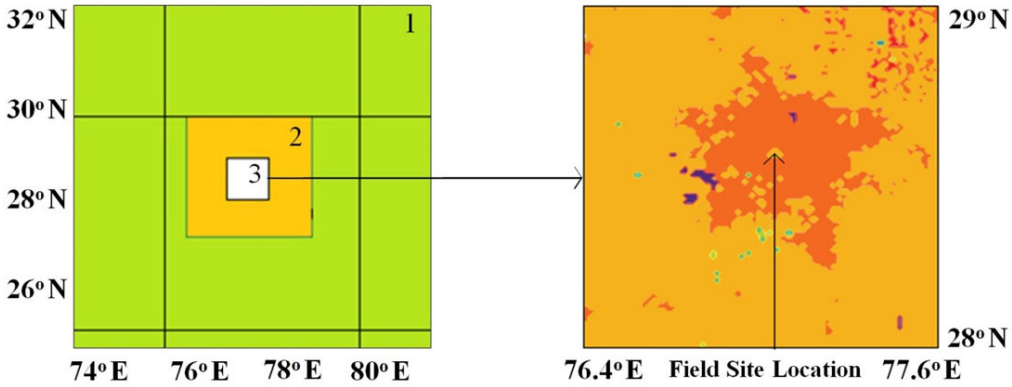


**Fig. 2**: (a) Nested domain and (b) location of field site at ICAR-IARI, New Delhi

***Field data***

A stand-alone SUCROS crop growth model was first calibrated and evaluated with observed data for spring wheat (cultivar HD2967) collected from an experimental site at the Indian Agricultural Research Institute (ICAR-IARI) campus in New Delhi. Dhakar, (2020) provided the data. The site is located at 28°08'N, 77°12'E. Data on phenology, growth and LAI at different developmental stages and yield of spring wheat were collected from the same experimental site. The observation-taking process is explained in (Kumari *et al.,* 2019). LAI data is available for three growing seasons: 2014-15, 2015-16 and 2016-17, while yield data is available for two years: 2015-16 and 2016-17. Meteorological data including, temperature, wind speed, incoming radiation, and vapor pressure, were also collected during the field experiment from an agrometeorological observatory near the experimental site.

***Gridded data used in WRF model***

In the WRF, MODIS land use data with 20 land categories with a spatial resolution of 30″ were used to interpolate topography and land use. The initial and boundary conditions were obtained from NCEP's final analysis data (NCEP-FNL), with a spatial resolution of 1° × 1°, operationally available at temporal intervals of 6 h. The FNL data parameters include sea level pressure, sea surface temperature, surface pressure, temperature, geopotential height,

**Table 2:** Irrigation dates.

| *YEAR* | *1st irrigation* | *2nd irrigation* | *3rd irrigation* | *4th irrigation* | *5th irrigation* |
|---|---|---|---|---|---|
| ***2014-15*** | *12 December* | *15 January* | *2 February* | *23 February* | *12 March* |
| ***2015-16*** | *10 December* | *6 January* | *16 February* | *2 March* | *18 March* |
| ***2016-17*** | *14 December* | *5 January* | *25 February* | *6 March* | *21 March* |

**Table 3:** Calibrated SUCROS coefficients for spring wheat.

| Calibrated Parameter | | Value |
|---|---|---|
| $T_{L1}$ | Thickness of 1st soil layer | 100 mm |
| $T_{L2}$ | Thickness of 2nd soil layer | 300 mm |
| $T_{L3}$ | Thickness of 3rd soil layer | 600 mm |
| $T_{L4}$ | Thickness of 4th soil layer | 1000 mm |
| $a_p$ | Rate of potential $CO_2$ assimilation at saturated light for individual | 0.0009636 g $CO_2$ $m^{-2}$ leaf $s^{-1}$ |
| $K_{df}$ | Extinction coefficient for leaves | 0.6 $m^2$ ground $ha^{-1}$ leaf |
| $e_{ff}$ | Factor showing initial light conversion for individual leaves | 12.0e-06 g $CO_2$ / J |
| $S_{cp}$ | Leaves scattering coefficient for PAR | 0.19 |
| $M_{lv}$ | Leaves Maintenance respiration coefficient | 0.03 g $CH_2O$ $g^{-1}$ DM $d^{-1}$ |
| $M_{st}$ | Stems maintenance respiration coefficient | 0.015 g $CH_2O$ $g^{-1}$ DM $d^{-1}$ |
| $M_{so}$ | Maintenance respiration coefficient of SO | 0.01g $CH_2O$ $g^{-1}$ DM $d^{-1}$ |
| $M_{rt}$ | Roots Maintenance respiration coefficient | 0.015 g $CH_2O$ $g^{-1}$ DM $d^{-1}$ |
| $a_{st}$ | Assimilate requirement for the production of stem dry matter | 1.413 g $CH_2O$ $g^{-1}$ DM |
| $a_{lv}$ | Assimilate requirement for the production of leaf dry matter | 1.463 g $CH_2O$ $g^{-1}$ DM |
| $a_{so}$ | Assimilate requirement for storage organ | 1.615 g $CH_2O$ $g^{-1}$ DM |
| $a_{rt}$ | Assimilate requirement for the production of root dry matter | 1.544 g $CH_2O$ $g^{-1}$ DM |
| $F_{cst}$ | Stem's mass fraction carbon | 0.647 g C $g^{-1}$ DM |
| r | Rate of relative growth of leaf area during crop's exponential growth | 0.01 °C $d^{-1}$ |
| $E_c$ | Constant for root elongation | 12 mm $d^{-1}$ |

soil values, relative humidity, ice cover, u- and v- winds, vertical motion, vorticity and ozone. The data was downloaded from the website: https://rda.ucar.edu/datasets/ds083.2/.

***Simulation domain & Model configuration***

The domain chosen to study crop-atmosphere interactions for spring wheat is centred around the observational field site. The phenological data at different growth stages and yield for spring wheat collected from the ICAR-IARI location were used to evaluate the WRF_NOAHMP_SUCROS coupled model. The WRF_NOAHMP_SUCROS simulation domains are shown in Fig. 2, and the details are provided in Table 1.

**Table 1:** Domain configuration

| Domain | Size | Resolution | Timestep |
|---|---|---|---|
| Parent domain | 900 km X 900 km | 9km X 9km | 27 |
| Nested domain 1 | 300 km X 300 km | 3km X 3km | 9 |
| Nested domain 2 | 100 km X 100 km | 1km X 1km | 3 |

The simulations were conducted for three seasons (2014-15, 2015-16 and 2016-17). The selection of simulation seasons was based on the availability of observed phenological data. The simulation period was from November 30 (approximate day of emergence) of first-year to April 15 of the next year. The model was integrated using a Runge-Kutta 3rd order scheme with time steps of 27, 9 and 3 seconds, respectively, for the 3 domains. Irrigation was applied by setting the soil moisture to 90% of the field capacity on the specified days. The irrigation days are shown in Table 2.

For all the simulations, boundary layer physics was from the Yonsei University scheme, surface layer physics was from the MM5 Monin-Obukhov scheme, cumulus physics was from the Kain-Fritsch scheme (turned off for finest domain), longwave and shortwave radiations were from the RRTMG scheme, and land surface physics is from Noah-MP land-surface scheme. The microphysics used is WRF Single-Moment (WSM) 3-class simple ice scheme. In dynamics, horizontal diffusion was determined with horizontal deformation using the Horizontal Smagorinsky first-order closure scheme.

## RESULTS AND DISCUSSION

***Calibration and validation of stand-alone SUCROS crop model***

SUCROS crop model was calibrated for spring wheat

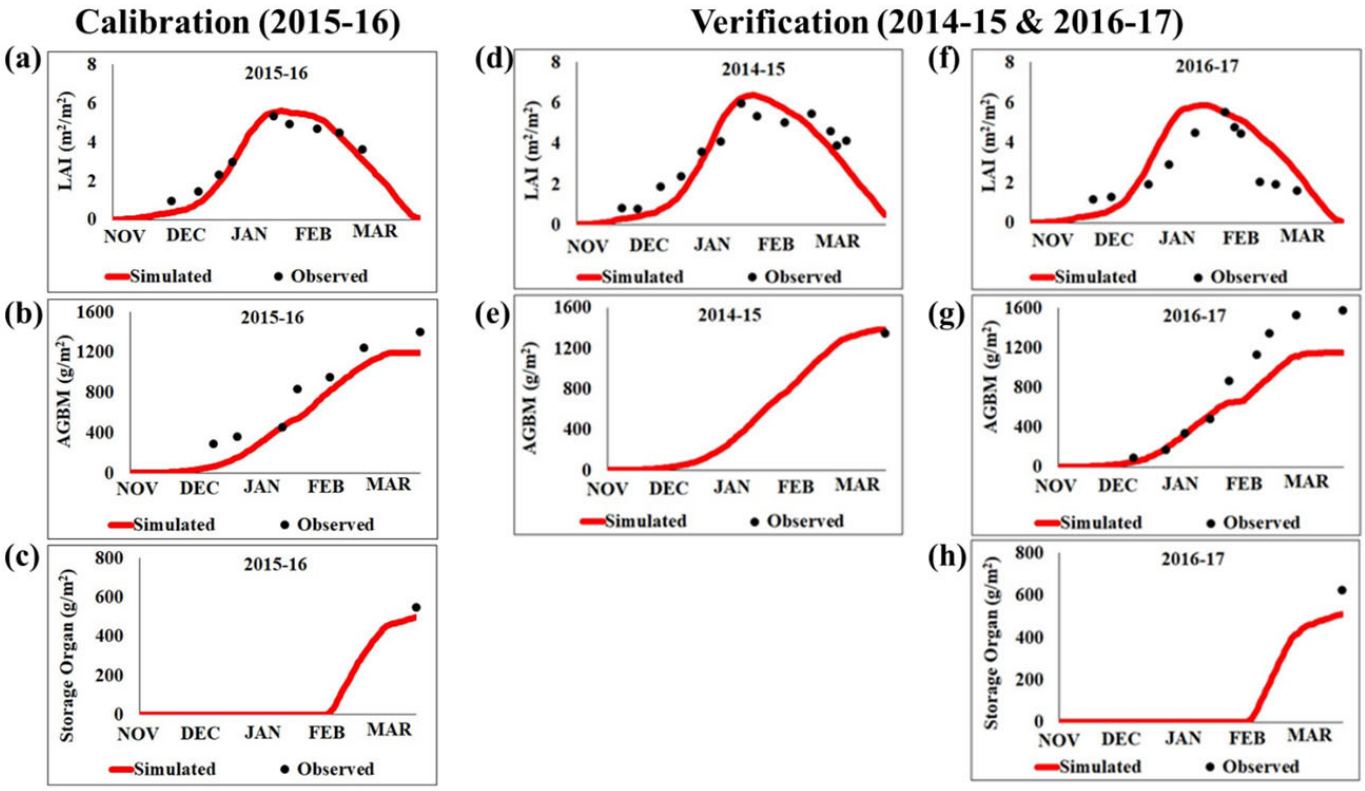


**Fig. 3:** Calibration of stand-alone SUCROS crop model for year 2015-16 (a) LAI (b) AGBM and (c) SO and validation for year 2014-15 (d - LAI and e - AGBM) and 2016-17 (f - LAI, g - AGBM and h – SO).

using LAI and yield data for 2015-16 and then validated against data for two different years, i.e., for 2014-15 and 2016-17. The calibration simulations were driven by daily mean temperature, vapor pressure, wind speed and total accumulated incoming radiation observed at the field site. The model was also initialized with observed soil moisture. Calibration involves finding an optimum combination of various SUCROS coefficients that best match the LAI and yield observations. First, a literature survey was undertaken to collect the appropriate coefficients. Multiple values were obtained for many coefficients. A UNIX shell script was devised to conduct SUCROS simulations with all the possible combinations and calculated various performance metrics, including bias, root mean square error and mean absolute error. The simulations were ranked based on the performance of the metrics, and the combination with the best average rank was selected. The selected combination was again fine-tuned to obtain the final set of values and has listed in Table 3.

Fig. 3 shows the calibration and validation of the stand-alone SUCROS crop model. The calibration is done for 2015-16, and verification is done for two years: 2014-15 and 2016-17. It shows that the calibrated model is performing quite well. The calibrated leaf area index, storage organ and above-ground biomass match well with the observed phenology for 2015-16. The validation results show that the temporal evolution of the simulated leaf area index closely matches the observed LAI for both evaluation years. The three-year simulated and observed LAI correlate well with a Pearson's correlation coefficient of 0.9 significant at $p < 0.001$. This suggests that the calibrated model is able to simulate the spring wheat crop phenology. The simulated above ground biomass matches the observed temporal pattern. The mass of the storage organ also approaches the final grain yield for the validation year 2016-17. However, these two parameters are underestimated by the SUCROS model.

***Validation of WRF_NOAHMP_SUCROS coupled model***

The following two simulations were performed for each year:

(a) NOAHMP_LAI simulation: Uncoupled model simulations using the WRF model with the default dynamic vegetation module in Noah-MP.

(b) WRF_NOAHMP_SUCROS simulation: Coupled model simulations using the WRF_NOAHMP_SUCROS model with the newly implemented dynamic vegetation module based on SUCROS.

Fig. 4 shows that the Noah-MP vegetation growth is dynamic, but as compared to observed data, the simulated leaf area index is unrealistic throughout the simulation period (NOAHMP_LAI). Even in the simulated runs, the days of emergence, maturity, and harvesting do not match crop phenology. We can analyse that the Noah-MP vegetation model (NOAHMP_LAI) cannot capture crop characteristics, so inadequate in performing land-atmosphere interaction studies.

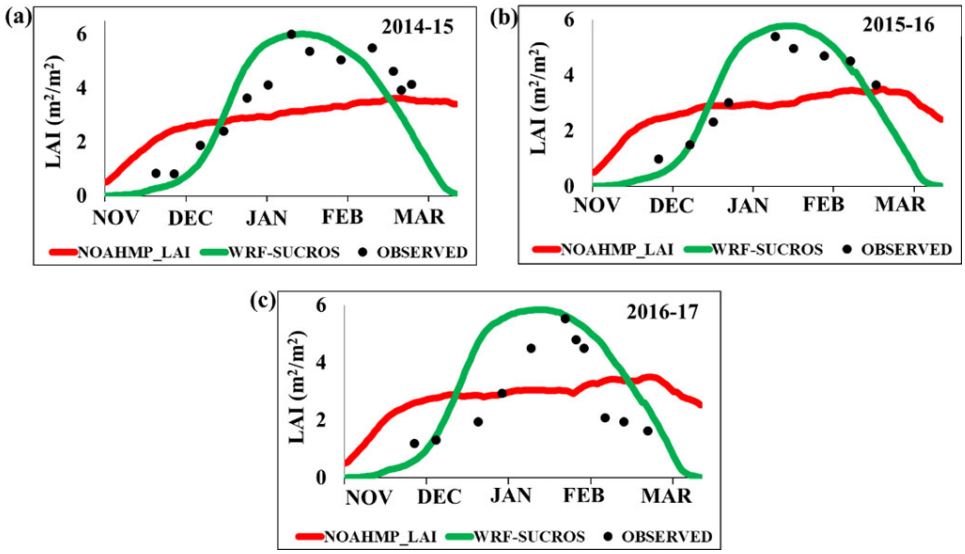


**Fig. 4:** WRF Noah-MP (NOAHMP_LAI) and dynamic coupled model (WRF_NOAHMP_SUCROS) simulated leaf area index for 2014-15 (a), 2015-16 (b) and 2016-17 (c) in comparison with observed leaf area index.

In WRF_NOAHMP_SUCROS simulations, the simulated leaf area index matches well with the ICAR-IARI observed leaf area index (Fig. 4). The simulated crop growth pattern follows the actual growth pattern with time. The day of emergence, maturity and harvesting information matches well with the observed phenomenon. The correlation coefficient between observed and simulated leaf area index in WRF_NOAHMP_SUCROS coupled model is 0.8144, and significance is < 0.0001. The above-ground biomass matches quite well with the observed biomass. The storage organ from the coupled model shows higher values than observed storage organs (Figures are not shown). Therefore, the newly developed coupled model can simulate all the interactions between crops and the atmosphere.

***Impact of dynamic crops on near-surface meteorology***

To understand the effect of vegetation dynamics on near-surface meteorology, we conducted the following two numerical experiments.

(i) WRF_NOAHMP_SUCROS: These simulations are conducted with the WRF_NOAHMP_SUCROS dynamic coupled model capable of simulating the two-way interactions between the croplands and the atmosphere. Here the SUCROS module calculates the LAI and root depth during the simulation using meteorological parameters simulated by WRF. The calculated LAI and root depth values are used to compute land properties and land-atmosphere fluxes of momentum, energy and moisture.

(ii) CLIM_LAI: These simulations are conducted with the most common WRF modelling approach using monthly mean climatological LAI values from MODIS data. The ICAR-IARI study site is categorized as urban in the MODIS database. Hence, instead of using MODIS data, I developed a monthly LAI climatology for the site using LAI taken from ICAR-IARI observations and then averaged monthly for December, January, February, March and April. Root depth was kept static in the model and equals to 1000 mm. In this approach, LAI is not affected by changes in meteorological conditions and hence one-way interaction only.

Thus, a comparison between these experiments will give us an idea about the effect of vegetation dynamics and two-way interactions on near-surface meteorology.

The sensitivity of land-atmosphere interactions in croplands is dependent on the leaf area index and root depth. The root depth helps in up taking water from different levels of the soil. The leaf area index calculates the entire fluxes that take place during crop growth. The leaf area index affects the evapotranspiration and is used to calculate the latent and sensible heat fluxes from the land surface. The sensible and latent heat fluxes have direct impacts on near-surface temperature and humidity. That is why I carefully compare the simulated LAI, latent and sensible heat fluxes and the near-surface temperature and mixing ratio to understand the effect of crop dynamics.

***Leaf area index***

Fig. 5(a) shows the simulated leaf area index for the WRF_NOAHMP_SUCROS simulation using the newly developed coupled model and the CLIM_LAI simulation using the uncoupled WRF model driven by climatological LAI. Fig. 5(f) shows the difference of LAI between the WRF_NOAHMP_SUCROS and CLIM_LAI. All simulations in Fig. 5 are averaged over three years (2014-15, 2015-16 and 2016-17) along with domain averages on cropland.

As discussed earlier, the WRF_NOAHMP_SUCROS model is computing the LAI from the meteorological parameters simulated by the WRF, so there is a dynamic variation throughout the season. In contrast, the LAI in CLIM_LAI is the climatology LAI developed using the LAI observed by ICAR-IARI and then averaged

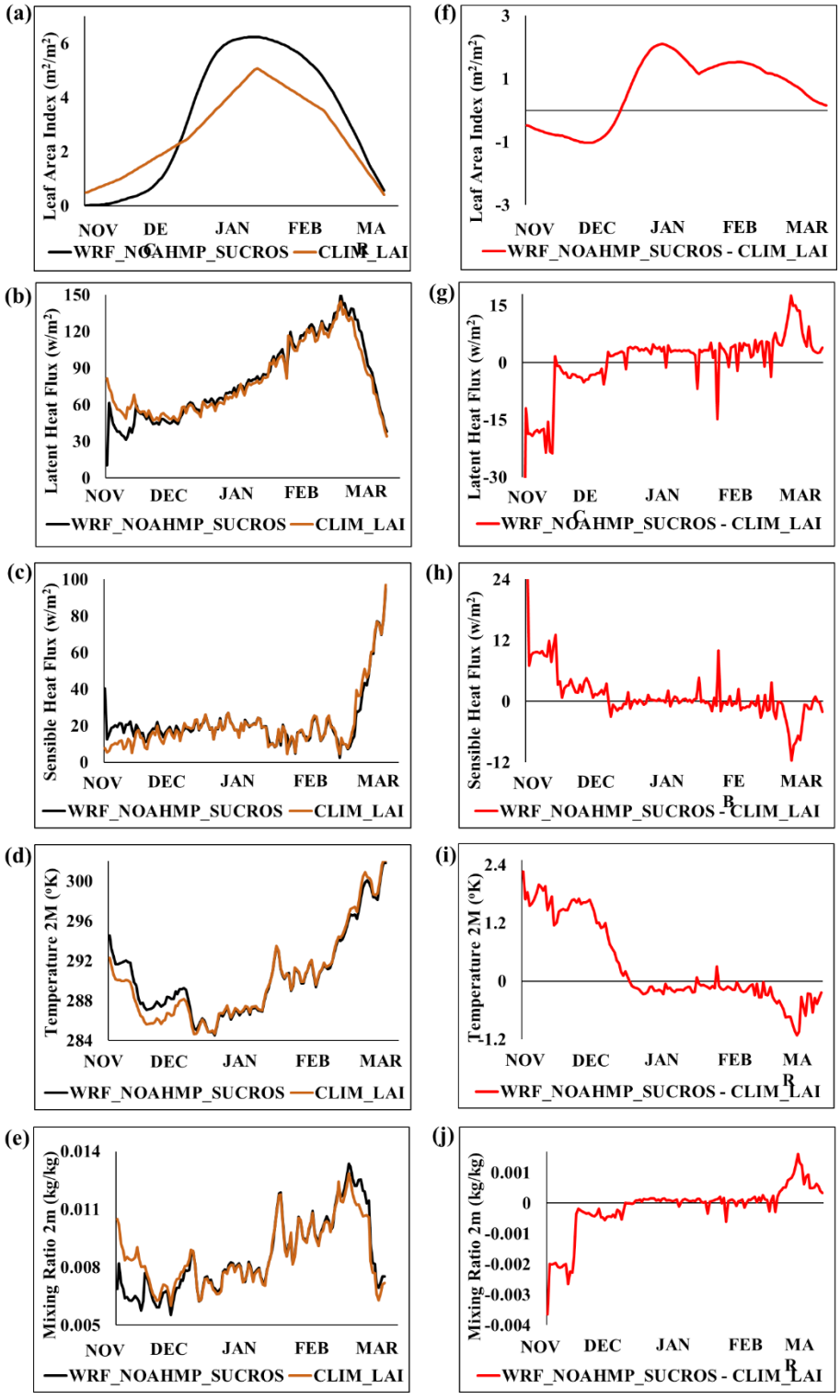


**Fig. 5:** (a) - (e) are the simulated values for LAI, LHF, SHF, temperature and mixing ratio, respectively, and (f) - (j) are the differences from WRF_NOAHMP_SUCROS for LAI, LHF, SHF, temperature and mixing ratio, respectively. All the individual plots are averaged over three years (2014-15, 2015-16 and 2016-17).

across the month. CLIM_LAI produces a linearly interpolated LAI over the entire season. During the initial phase, as the LAI starts to rise concerning the development stage, the difference is showing negative values in January, but in February, during the peak LAI, there is a sharp change in CLIM_LAI compared to the WRF_NOAHMP_SUCROS LAI, which gives a decline. Again, in March and April, the LAI decreases due to ageing and the self-shading factor in both cases, so the difference approaches zero.

***Latent heat flux***

Latent heat flux varies directly with LAI. As LAI increases, the latent heat flux increases, and as LAI decreases, it will decrease latent heat flux. As the crop grows, the LAI tends to increase. Due to the increased LAI, the stomatal conductance will be higher (Pitman, 2003), i.e. there will be more water loss during $CO_2$ intake, which will help in energy transfer in the form of latent heat flux compared to sensible heat flux.

The simulated latent heat flux is shown in Fig. 5(b). During the initial stages, the leaf area index is high in the case of CLIM_LAI compared to WRF_NOAHMP_SUCROS [Fig. 5(a)] due to which the latent heat is higher in CLIM_LAI case as compare to WRF_NOAHMP_SUCROS in the beginning.

The latent heat flux is less in WRF_NOAHMP_SUCROS but still has non-zero values during the initial stage. This can be due to more evaporation at the bare ground because of the availability of sufficient soil moisture and high radiation.

During the Juvenile stage, as the plant grows, the LHF also increases due to increased LAI. From the difference plot [Fig. 5(g)], we can see that the latent heat flux is negative as LAI is negative. But as the LAI increases (WRF_NOAHMP_SUCROS), the latent heat also increases positively. The difference is small but also not negligible. The reason behind the small difference value is the dominance of soil moisture. The minimum water stress factor helps in more latent heat flux even if the LAI is small. Also, the temperature cools down under vegetated areas, slowing down the impact of radiation and decreasing evapotranspiration and latent heat flux.

This can be one reason for less difference value in WRF_NOAHMP_SUCROS and CLIM_LAI experiment even if WRF_NOAHMP_SUCROS has more LAI. If we talk about some more possible reasons behind closer values during the juvenile stage, there are two main factors are affecting the evapotranspiration in the model: Firstly, for the experiments, I have applied the two-stream radiation transfer scheme. The vegetation is considered with the gaps over the grid-cells to avoid too many shadows in the vegetated area. The evapotranspiration in this is due to the transpiration from the vegetation leaves and evaporation from the ground to canopy under vegetation and bare ground. So, the total evapotranspiration is the sum of transpiration, evaporation over canopies, evaporation over vegetated ground and over bare ground.

The second reason is that root depth plays an important role in transpiration. In the WRF_NOAHMP_SUCROS experiment, the root depth is dynamic and varies as the plant grows, but in CLIM_LAI experiment, the root depth is static and fixed to 1000 mm at every plant stage that helps in maximum transpiration.

During the mature stage, the difference of (WRF_NOAHMP_SUCROS-CLIM_LAI) is not negative, the LHF also shows an increase during the mature stage, and as LAI starts dying due to the ageing factor, the LHF also varies accordingly. Thus, the impact of the dynamic crop can be clearly seen in the case of latent heat flux variation.

As both the experiments have almost similar LAI, as shown in Fig. 5(a), from Fig. 5(g), the difference of impact of vegetation on latent heat flux is a little bit small and ne eds a clearer picture to understand.

Therefore, to understand the impact of vegetation on latent heat flux, here the latent heat flux was divided into four different modes by which latent heat flux transfer takes place. The total latent heat flux is the sum of transpiration, evaporation over the canopy, evaporation over bare ground and evaporation over the vegetated ground. The impact caused by these different modes is shown in Fig. 6.

It is a well-known fact that transpiration takes place from the leaves of plants during photosynthesis and is entirely based on the plant growth, i.e. leaf area index. It is clear from Fig. 6(a) that transpiration is high when the leaf area index is high and vice versa. The difference plot 6(e) follow the leaf area index difference pattern from Fig. 5(f). The peaks show the events of irrigation and rainfall.

From the figure, we can analyse that WRF_NOAHMP_SUCROS has less latent heat flux than CLIM_LAI during the initial phase because it has a smaller LAI. But as the LAI increases in the juvenile and mature stages, the latent heat flux increases in WRF_NOAHMP_SUCROS and has a value higher than CLIM_LAI.

Another evaporation mode is evaporation on the canopy, which is also affected by the leaf area index, as shown in Fig. 6(b). Evaporation on the canopy occurred when it rained. The rain causes an interception of water on the plant's leaves and helps evaporation over the canopy. The more LAI, the more evaporation on the canopies and vice versa. This can be clearly seen from the difference plots in Fig. 6(f). The negative values in the difference plots show that the precipitation captured in the CLIM_LAI experiment is higher than that of WRF_NOAHMP_SUCROS.

When we talk about the third way of transfer of latent heat flux, i.e., evaporation on the vegetated ground. As discussed earlier, vegetation is considered with gaps in between so that it can avoid too much overlapping of plants and hence shade. In this case, evaporation occurs on the ground under the vegetation. Direct or diffused radiation goes under the vegetation zone and helps evaporation.

The evaporation on bare ground, if the ground is exposed to direct radiation, i.e., when there is no plant, or we can say no leaf area index, then evaporation will be high, but if in any case, the plant exists with some value of leaf area index, evaporation will be reduced by the leaf area index as it will reduce the radiation reaching the ground. This can be seen in Fig. 6(c) & 7(g).

Similarly, in case of evaporation on the vegetated ground is shown in Fig. 6(d). When the leaf area index is low, radiation in any form (either direct or diffuse) can penetrate beneath the plants and help in more evaporation. When the leaf area index is high, the effect of radiation on the vegetated ground is reduced, and hence evaporation is also reduced, as shown in the difference plot Fig. 6(h).

So, here it is seen that the evaporation mode is different

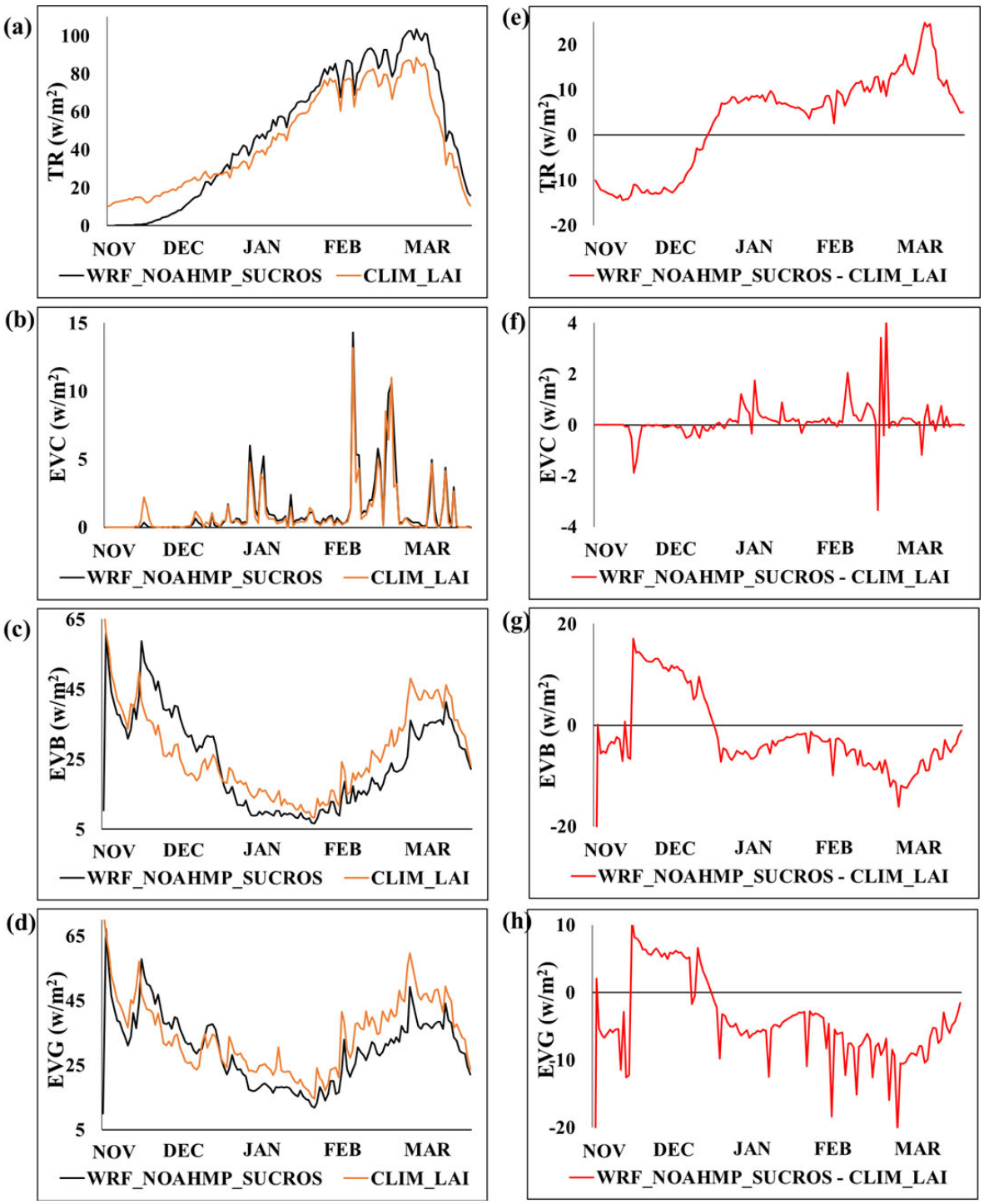


**Fig. 6**: Evapotranspiration representations averaged over three years. (a) to (d) are showing the simulated evaporation over vegetation, canopies, bare ground and vegetated ground for WRF_NOAHMP_SUCROS and CLIM_LAI and (e) to (h) showing respective evaporation differences of CLIM_LAI from WRF_NOAHMP_SUCROS.

for all the experiments, but the summation amount is almost the same (Fig. 5b) under no water stress conditions.

***Sensible heat flux***

In a previous discussion, we saw that how latent heat fluxes relate to crop dynamics. So, after latent heat flux, the simulated sensible heat flux is shown in Fig. 5(c). Over crops, the sensible heat flux behaves just opposite to latent heat flux. When LAI is less sensible heat flux is more and vice-versa. During initial stage, as the ground is clear in WRF_NOAHMP_SUCROS compared to CLIM_LAI, more radiation reaches the ground, making the lower surface hotter. The energy transfer takes place in the form

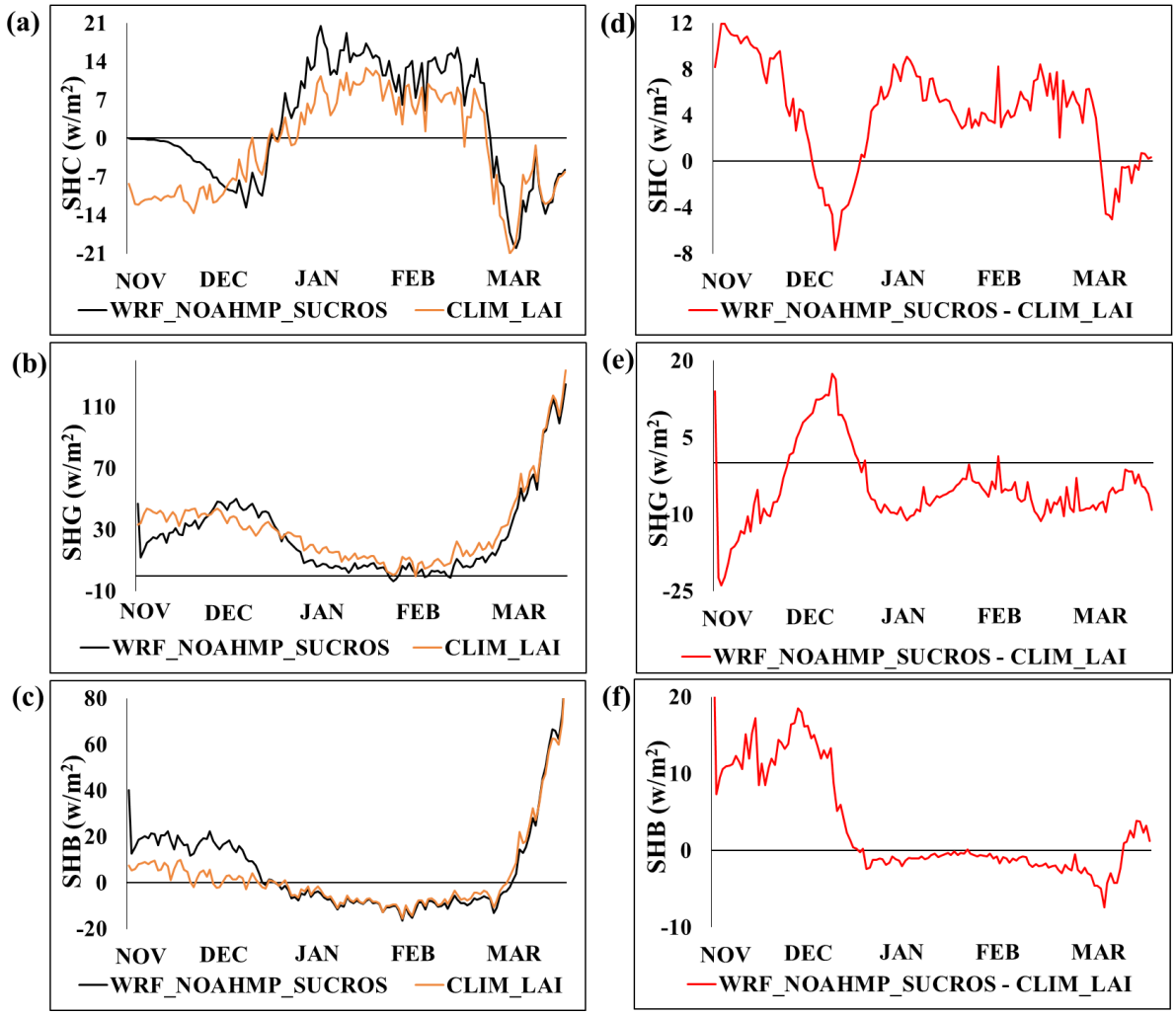


**Fig. 7:** Sensible heat flux representations averaged over three years. (a) to (c) are showing the simulated evaporation over canopies, vegetated ground and bare ground for WRF_NOAHMP_SUCROS and CLIM_LAI and (d) to (f) showing respective evaporation differences of CLIM_LAI from WRF_NOAHMP_SUCROS.

of sensible than in latent heat flux. But as the crop growth takes place, the sensible heat is lower down by latent heat flux because of more evapotranspiration over crops, and also when irrigation and precipitation take place, there is a sharp decrease in sensible heat flux as increased soil moisture leads to more evapotranspiration. During the mature stage, as the plants begin to die, the impact of LAI dominates here. The decreased leaf area index results in decreased latent heat flux and increased sensible heat flux. From the difference plot [Fig. 5(h)], it is clear that when LAI is non-negative in WRF_NOAHMP_SUCROS-CLIM_LAI, the LHF is more and the sensible heat flux follows the just reverse pattern. The above discussions clearly show that the LAI is the dominant factor during the initial and mature stages. Whereas during the juvenile stage, there are many factors that impact energy fluxes non-linearly.

Energy transfer occurs in the form of latent heat and sensible heat. There is a balance between these two forms. When the energy transfer is in the form of latent heat flux, it means that the energy transfer will be less in the form of sensible heat flux and vice versa. Therefore, in order to understand energy transfer in crops, the various forms of latent heat flux are described. Now to make it more understandable, the sensible heat flux is divided into its various parts so that it can more precisely describe the importance of the dynamic vegetation. In the cropland area, sensible heat flux occurs over canopies, vegetated ground and bare ground.

Fig. 7 is representing the sensible heat flux over the canopies (SHC), vegetated ground (SHG) and bare ground (SHB). Here it can be clearly seen that during the initial phase of WRF_NOAHMP_SUCROS and CLIM_LAI, both have negative sensible heat flux (Fig 7(a)). CLIM_LAI has more negative values than WRF_NOAHMP_SUCROS because CLIM_LAI has higher LAI during initial stages than WRF_NOAHMP_SUCROS so it will have more energy transfer as latent heat flux than sensible heat flux whereas WRF_NOAHMP_SUCROS has lower leaf area index, so energy transfer as latent heat flux will be less and in that case energy transfer will be in the form of sensible heat.

That's why the WRF_NOAHMP_SUCROS model shows

fewer negative numbers than CLIM_LAI during the initial phase. As the crop progresses during the mature stage, WRF_NOAHMP_SUCROS still has a more sensible heat flux. Above the canopy, when rain events occur, and water stagnates over the leaves, sensible heat flux is disrupted. But when there is no water on the leaves, energy transfer will take place in the form of sensible heat.

When it rains, there is a sharp change in the sensible and latent heat fluxes. Furthermore, during the fully developed plant stages, the temperature cools down, thereby reducing evaporationtranspiration and hence latent heat flux. Thus energy transfer occurs in the form of sensible heat flux to maintain the radiation balance. This is why WRF_NOAHMP_SUCROS has more latent and sensible heat flux over the canopies.

The effect of vegetation can be clearly seen if we talk about sensible heat flux on the vegetated ground and bare ground. When the leaf area index is high, the penetration of radiation beneath the plants will be somewhat difficult, leading to less energy transfer. And when the leaf area index is low, the sensible heat flux will be high. This effect can be clearly seen in Fig. 7 (b,c,e & f).

***Near-surface temperature***

The near-surface air temperature varies directly with sensible heat flux. During the emergence, because of negligible LAI, the heat transfer takes place in form of sensible heat flux in contrast to latent heat flux that results in a warmer effect over the croplands [Fig. 5(d) & 5(i)]. The growing crops results in near surface cooling due to decreased Bowen Ratio. As the crop dies, the temperature increases because of increasing sensible heat and provides a warming effect again during the harvesting stage over croplands.

*Mixing ratio*

The simulated mixing ratio patterns are shown in Fig. 5(e). The mixing ratio is more when the mass of water contained in the air is more. So, the mixing ratio directly varies as the latent heat flux. When LHF is more, the mixing ratio is also more and vice-versa. From difference plots [Fig. 5(j)] it is clear that in the case of (WRF_NOAHMP_SUCROS-CLIM_LAI), the mixing ratio is negative during the initial stage as LAI is also negative, but it is positive when LAI is positive during the mature stage.

As we saw from the above simulations that dynamic vegetation has a well-proven effect on near-surface meteorology, and even for forecast simulations, we cannot provide the observed data, so we need a model that can simulate dynamic vegetation and simulate the associated near-surface meteorology.

## CONCLUSION

The study focused on looking at the impact of dynamic vegetation on land surface-atmosphere interactions on spring wheat cropland in India. A new coupled model WRF_NOAHMP_SUCROS was developed to study these interactions by incorporating the crop growth module of the SUCROS crop model into the Noah-MP land module of the WRF mesoscale model that exchanges information and calculates different water and energy flows. In an earlier study, the stand-alone SUCROS crop growth model was calibrated and evaluated with observed data for spring wheat (cultivar HD2967) collected from an experimental site at the Indian Agricultural Research Institute (ICAR-IARI) campus in New Delhi. The crop growth module of the calibrated SUCROS model was implemented in the Noah-MP land module of the WRF model. Numerical experiments were conducted with the coupled WRF_NOAHMP_SUCROS model to simulate the simultaneous evolution of the meteorology and crop phenology over the study area for the 2014-15, 2015-16 and 2016 -17 growing seasons.

Results show that the coupled WRF_NOAHMP_SUCROS model can simulate the temporal evolution of LAI that matches well with the observed crop growth. The performance of the coupled model is better than the default dynamic vegetation module in WRF that overestimates LAI in the beginning and end of the growing season but underestimates the LAI peak.

The impact of dynamic vegetation can be clearly seen in the surface meteorological parameters simulated by WRF_NOAHMP_SUCROS. The latent heat flux varies directly with LAI, and sensible heat flux varies inversely with LAI. As the crop grows the energy transfer takes place more in the form of latent heat flux than sensible heat flux. Hence the growing crops result in near-surface cooling while the increased latent heat flux results in an increased mixing ratio.

Simulations with the uncoupled WRF model driven by observed LAI that does not simulate the two-way interactions also match the LAI patterns. However, in the juvenile crop stage it overestimates the sensible heating and temperature but underestimates latent heat fluxes and mixing ratio.

Upon further calibration, the WRF_NOAHMP_SUCROS model can be used over different kinds of agro-ecosystems to simulate the simultaneous evolution of meteorological drivers and crop phenology. The dynamic coupling allows us to simulate two-way interactions between croplands and the atmosphere. Simulating such interactions are not possible with static or non-interactive vegetation that is typically used in mesoscale modeling. Thus, the coupled model and the coupled modeling approach can be a valuable tool for simulating and understanding processes occurring in the Earth System.

## ACKNOWLEDGEMENTS

This work was funded by the Science and Engineering Research Board, Department of Science and Technology, Govt. of India, grant number SB/S4/AS-146/2014.

***Conflict of Interest Statement:*** The author(s) declare(s) that there is no conflict of interest.

***Disclaimer***: The contents, opinions, and views expressed in the research article published in the Journal of Agrometeorology are the views of the authors and do not necessarily reflect the views of the organizations they belong to.

***Publisher's Note:*** The periodical remains neutral with regard to jurisdictional claims in published maps and institutional affiliations.

## REFERENCES


Asseng, S., Ewert, F., Martre, P., Rötter, R.P., Lobell, D.B., Cammarano, D., Kimball, B.A., Ottman, M.J., Wall, G.W., White, J.W., Reynolds, M.P., Alderman, P.D., Prasad, P.V.V., Aggarwal, P.K., Anothai, J., Basso, B., Biernath, C., Challinor, A.J., Sanctis, G. De, Doltra, J., Fereres, E., Garcia-Vila, M., Gayler, S., Hoogenboom, G., Hunt, L.A., Izaurralde, R.C., Jabloun, M., Jones, C.D., Kersebaum, K.C., Koehler, A-K., Müller, C., Naresh Kumar, S., Nendel, C., O'Leary, G., Olesen, J.E., Palosuo, T., Priesack, E., Eyshi Rezaei, E., Ruane, A.C., Semenov, M.A., Shcherbak, I., Stockle, C., Stratonovitch, P., Streck, T., Supit, I., Tao, F., Thorburn, P.J., Waha, K., Wang, E., Wallach, D., Wolf J., Zhao, Z., Zhu, Y. (2015). Rising temperatures reduce global wheat production. *Nat. Clim. Chang.*, 5(2), 143-147, doi:10.1038/nclimate2470.

Avissar, R. and Verstraete, M.M. (1990). The representation of continental surface processes in mesoscale atmospheric models. *Rev. Geophys*., 28, 35–52.

Ball, J. T., Woodrow, I. E., Berry, J. A. (1987). A model predicting stomatal conductances and its contribution to the control of photosynthesis under different environmental conditions. In: Progress in Photosynthesis Research, (ed J. Biggins), *Martinus Nijhoff, Dordrecht,* 4, 221-224.

Bonan, G., Levis, S., Sitch, S., Vertenstein, M., Oleson, K. (2003). A dynamic global vegetation model for use with climate models: Concepts and description of simulated vegetation dynamics. *Glob. Chang. Biol*., 9(11), 1543-1566. doi: 10.1046/j.1365-2486.2003.00681.x.

Campo, L., Castelli, F., Entekhabi, D., Caparrini, F. (2009). Land atmosphere interactions in a high-resolution atmospheric simulation coupled with a surface data assimilation scheme. *Nat. Hazards Earth Syst. Sci*., 9, 1613-1624, doi:10.5194/ nhess-9- 1613-2009.

Chen, F., Xie Z. (2011). Effects of crop growth and development on land surface fluxes, *Adv. Atmos. Sci.*, 28(4), 927-944, DOI: 10.1007/s00376-010-0105-1.

Chen, Ying , Feng-Shan Liu, Fu-Lu Tao, Quan-Sheng Ge, Min Jiang, Meng Wang, Feng-Hua Zhao (2020). Calibration and validation of SiBcrop Model for simulating LAI and surface heat fluxes of winter wheat in the North China Plain. *J. Integ. Agric.,* 19(9): 2206-2215.

Dan, L., Ji, J., Li, Y.P. (2005). Climatic and biological simulations in a two-way coupled atmosphere-biosphere model (CABM). *Glob. Planet. Change.*, 47, 153–169.

De Fries R.S., Foley J.A., Asner, G.P. (2004). Land-use choices: balancing human needs and ecosystem function*. Front. Ecol. Environ*., 2, 249–257.

Dhakar R. (2020). Regional wheat yield prediction using remote sensing inputs with dynamic crop-weather models. Ph.D. Thesis submitted to Division of Agricultural Physics, ICAR-Indian Agricultural Research Institute, New Delhi India, pp.209.

Dickinson, R.E., Shaikh, M., Bryant, R., Graumlich, L. (1998). Interactive canopies for a climate model. *J. Clim*., 11, 2823–2836.

Foley, J.A., Costa, M.H., Delire, C., Ramankutty, N., Snyder P. (2003). Green surprise? How terrestrial ecosystems could affect earth's climate. *Front. Ecol. Environ*., 1, 38–44.

Foley, J.A., Levis, S., Prentice, I.C., Polaard, D., Thompson, S.L. (1998). Coupling dynamic models of climate and vegetation, *Glob Chang Biol.,* 4, 561–79.

Goudriaan, J., van Laar, H. H. (1994). Modelling Potential Crop Growth Processes. 2nd ed., 274, Kluwer, Dordrecht, Netherlands.

Harding, K.J., Twine, T.E., Lu, Y. (2015). Effects of dynamic crop growth on the simulated precipitation response to irrigation. *Earth Interact*., 19, 1–31.

Hatfield, J. L., Prueger, J. H. (2015). Temperature extremes: Effect on plant growth and development. *Weather. Clim. Extremes*, 10(A) 4-10, https://doi.org/10.1016/j.wace.2015.08.001,

Hatfield, J.L., Boote, K.J., Kimball, B.A., Ziska, L.H., Izaurralde, R.C., Ort, D., Thomson, A.M., Wolfe, D.W. (2011). Climate impacts on agriculture: implications for crop production. *J. Agron.,* 103, 351-370.

Henderson-Sellers, A., McGuffie, K. (1995). Global climate models and 'dynamic' vegetation changes. *Glob. Chang. Biol.,* 1(1), 63-75, doi.org/10.1111/j.1365-2486.1995.tb00007.x.

Hundal, S.S., Prabhjyot-Kaur. (2007). Climatic variability and its impact on cereal productivity in Indian Punjab: A simulation study. *Curr. Sci*., 92(4)**:** 506–511.

Jiang, X., Niu, G.-Y., Yang, Z.-L. (2009). Impacts of vegetation and groundwater dynamics on warm season precipitation over the Central United States. *J. Geophys. Res*., 114, D06109, doi:10.1029/2008JD010756.

Kumari, S., Baidya Roy, S., Sharma, P., Srivastava, A., Sehgal, V. K., Dhakar, R. (2019). Modeling impacts of climate change on spring wheat in northern India. *J. Agrometeorol*., 21(2), 123-130. https://doi.org/10.54386/jam.v21i2.222

Lambin, E.F., Geist, H.J., Lepers, E. (2003). Dynamics of land-use and land cover change in tropical regions*. Annu. Rev. Environ. Resour.*, 28, 205–241.

Liu, X., Chen, F., Barlage, M., Zhou, G., Niyogi, D. (2016). Noah-MP-Crop: Introducing dynamic crop growth in the Noah-MP land surface model. *J. Geophys. Res. Atmos.*, 121, 13,953–13,972, doi:10.1002/ 2016JD025597.

Lu, L., Pielke, R.A., Liston, G.E., Parton, W.J., Ojima, D., Hartman,

M. (2001). Implementation of a two-way interactive atmospheric and ecological model and its application to the central United States. *J. Clim*., 14, 900-919.

Lu, Y., Jin, J., Kueppers, L.M. (2015). Crop growth and irrigation interact to influence surface fluxes in a regional climate-cropland model (WRF3. 3-CLM4crop). *Clim. Dyn*., 45, 3347–3363.

Niu, G.Y., Yang, Z.L.(2004). Effects of vegetation canopy processes on snow surface energy and mass balances, *J. Geophys. Res*., 109, D23111, doi:10.1029/2004JD004884.

Niu, G.Y., Yang, Z.L., Mitchell, K.E., Chen, F., Ek, M.B., Barlage, M., Kumar, A., Manning, K., Niyogi, D., Rosero, E., Tewari, M., Xia, Y. (2011). The community Noah land surface model with multiparameterization options (NoahMP): 1. Model description and evaluation with local scale measurements. *J. Geophys. Res. Atmos.,* 116(D12).

Osborne, T., Slingo, J., Lawrence, D., Wheeler, T. (2009). Examining the interaction of growing crops with local climate using a coupled crop-climate model. *J. Clim*., 22, 1393–1411.

Osborne, T.M., Lawrence, D.M., Challinor, A.J., Slingo, J.M., Wheeler, T.R. (2007). Development and assessment of a coupled crop-climate model. *Glob. Chang. Biol*., 13(1), 169-183, doi: 10.1111/j.1365-2486.2006.01274.x.

Pandey, V., Patel, H.R., Patel, V.J. (2007). Impact assessment of climate change on wheat yield in Gujarat using CERES-wheat model. *J. Agrometeorol*., 9(2), 149–157. https://doi.org/10.54386/jam.v9i2.1122

Pielke, R.A., Avissar, R., Raupach, M., Dolman, A.J., Zeng, X.B., Denning, A.S. (1998). Interactions between the atmosphere and terrestrial ecosystems: influence on weather and climate. *Glob. Chang. Biol.*, 4: 461–475.

Pitman, A.J. (2003). The evolution of, and revolution in, land surface schemes designed for climate models. *Int. J. Climatol*., 23(5), 479–510.

Sacks, W.J., Kucharik, C.J. (2011). Trends in crop management and phenology in the U.S. Corn Belt, and impacts on yields, evapotranspiration, and energy balance. *Agric. For. Meteorol.*, doi: 10.1016/j.agrformet.2011.02.010.

Scanlon, B.R., Reedy, R.C., Stonestrom, D.A., Prudic, D.E., Dennehy, K.F. (2005). Impact of land use and land cover change on ground water recharge and quality in the southwestern US. *Glob. Chang. Biol*., 11, 1577–1593.

Sellers, PJ. (1992). Biophysical models of land surface processes. In Climate System Modelling, Trenberth KE (ed.), Cambridge University Press.

Shin, D.W., Bellow, J.G., LaRow, T.E., Cocke, S., O'Brien J. J. (2006). The role of an advanced land model in seasonal dynamical downscaling for crop model application. *J. Appl. Meteorol. Climatol.,* 45, 686-701.

Tsarouchi, G.M., Buytaert, W., Mijic, A. (2014). Coupling a land-surface model with a crop growth model to improve ET flux estimations in the Upper Ganges basin, India. *Hydrol. Earth Syst. Sci.,* 18, 4223–4238.

Tsvetsinskaya, E.A., Mearns, L.O., Easterling, W.E. (2001a). Investigating the effect of seasonal plant growth and development in three-dimensional atmospheric simulations. Part I: Simulation of surface fluxes over the growing season. *J. Clim*., 14, 692–710.

Twine, T.E., Kucharik, C.J., Foley, J.A. (2004). Effects of land cover change on the energy and water balance of the Mississippi River basin. *J. Hydrometeorol*., 5, 640–655.

Van den Hoof, C., Vidale, P.L., Hanert, E. (2011). Simulating dynamic crop growth with an adapted land surface model – JULES-SUCROS: model development and validation. *Agric. For. Meteorol*., 151, 137-153, doi: 10.1016/j.agrformet.2010.09.011.

Yang, Z.L., Niu, G.Y. (2003). The versatile integrator of surface and atmosphere processes: Part 1. Model description, *Glob Planet Change*, 38, 175–189.

Yao, F., Xu, Y., Lin, E., Yokozawa, M., Zhang, J. (2007). Assessing the impacts of climate change on rice yields in the main rice areas of China. *Clim. Change*, 80, 395–409 https://doi.org/10.1007/s10584-006-9122-6.

Zou, J., Xie, Z., Zhan, C., Chen, F., Qin, P., Hu, T., Xie, J. (2019). Coupling of a Regional Climate Model with a Crop Development Model and Evaluation of the Coupled Model across China. *Adv. Atmos. Sci*., 36, 527–540, https://doi.org/10.1007/s00376-018-8160-0.